OFDM: An Old Idea Solves New Problems

Karl-Dirk Kammeyer and Heiko Schmidt
University of Bremen, FB-1,
P.O. Box 33 04 40, D-28334 Bremen, Germany,
e-mail: kammeyer@comm.uni-bremen.de
and
Reinhard Rückriem and Stefan Fechtel
Infineon Technologies AG,
P.O. Box 80 09 49, D-81609 Munich, Germany
e-mail: reinhard.rueckriem@infineon.com

Abstract—***The multicarrier technique is known since more than 40 years. First practical applications, however, were not considered before 1990 when Bingham's famous paper appeared which pointed out the great attraction of this idea – especially in the form of the FFT-based "OFDM" (Orthogonal Frequency Division Multiplexing). Meanwhile, OFDM is applied in the DAB and DVB standard (Digital Audio/Video Broadcasting) and in modern indoor communication concepts like HIPERLAN/2 and IEEE802.11a. In this paper an overview of new techniques in the field of multicarrier transmission will be given. At first, the attention is focused on the problems of equalization and channel estimation. Noise reduction methods are applied which exploit the fact that the channel impulse response is shorter than the FFT length used. A quite modern concept is the so-called "turbo estimation" where channel decoding can be included in the estimation process. This leads to a very powerful channel tracking algorithm. In some recent papers OFDM was compared to the classical single carrier structure with a frequency domain equalizer; here it will shown that OFDM outperforms the single carrier structure if channel coding is taken into account. The performance of the algorithms developed here is demonstrated by simulation results based on the HIPERLAN/2 Standard.***

Keywords— ***OFDM, multicarrier transmission, HIPERLAN, channel estimation, turbo estimation, channel tracking, impulse shortening equalizer, frequency domain equalizer.***

I. Historical Background

The fundamental idea of multicarrier transmission was born in 1957 when M. Doelz presented a new data transmission method which he called "KINEPLEX" [1]. Ten years later, Saltzberg's paper [2] appeared which applied a specific overlapping impulse shaping concept – in this paper also a theoretical orthogonal Nyquist shaping based on Offset QAM was derived. The technique which we today call "OFDM" (Orthogonal Frequency Division Multiplexing) was introduced in 1971 by Weinstein and Ebert [3]; here for the first time, the efficient DFT structure was presented. Since 1971, the OFDM technique was re-invented several times – e.g. [4], [5] – even a hardware realization was presented in [6]. At that time, however, no commercial applications were considered. The break-through came with the well-known Bingham paper [7] – probably the non-conventional title attracted the attention of communication people. Beside the usual DFT-based OFDM system some authors studied more general concepts using either time-overlapping or spectral-overlapping impulses (e.g. gaussian impulses which are characterized by their minimum time-bandwidth property) [9], [10], [11], [12], [13]. In that case, intersymbol interference (ISI) or inter carrier interference (ICI), respectively, are removed by Viterbi equalization.

The first important application of the multicarrier technique was considered in the Digital Audio Broadcast (DAB) concept and later in Digital Video Broadcasting (DVB) [14], [15], [16]. It should be mentioned that for the 3rd generation standard UMTS (Universal Mobile Telecommunication System), OFDM was among the concepts proposed [17]. However, it was not accepted. Currently, new systems for indoor communications are under preparation: the new W-LAN standards HIPERLAN/2 and IEEE802.11a are based on the OFDM technique [18], [19].
Beside the applications in wireless communications, multi carrier solutions are also introduced in ADSL (Asymmetric Digital Subscriber Line) and HDSL (High-Speed Digital Subscriber Line) – in these applications it is usually denoted as DMT (Discrete Multi Tone) [20] instead of OFDM – this is just a different name, the technique is quite the same.

This paper is organized as follows. After an introduction into the fundamentals of OFDM, the important problem of channel estimation is addressed in section III; noise reduction techniques as well as the modern "turbo estimation" principle are applied – the latter technique leads to an efficient channel tracking algorithm which solves the problems arising from long data bursts under time variant conditions in section IV. The channel estimation is considered under the specific condition that some subcarriers are unmodulated as it is the case e.g. in HIPERLAN/2. In some recent papers OFDM is opposed to the similar looking structure of a classical single carrier technique with a frequency domain equalizer; in section V both concepts are compared under channel coding conditions. The guard interval introduced in the OFDM signal must be longer than the maximal duration of the channel echos; if this condition is violated ISI occurs. To overcome this problem linear pre-equalizers can be applied for impulse shortening the design of which is discussed in section VI. The performance is demonstrated by simulation results on conditions of the HIPERLAN/2 standard. Finally, a conclusion is given which summarizes the main results of this paper.

II. The Principles of Multicarrier Transmission

Primarily, the multicarrier technique OFDM can be described as an analog discrete multi-tone filterbank with rectangular (orthogonal) impulse shaping filters for each subcarrier. Figure 1 depicts a basic OFDM block diagram. Each complex data sym-

bol $d_n(i)$ is mapped onto the n^{th} among N subcarriers, where i denotes the current time slot or OFDM symbol. Practically, discrete transmitter and receiver filter banks are used and computed efficiently by FFT algorithms. The complex OFDM time domain baseband symbol is

$$s(i,k) = \sum_{n=0}^{N-1} d_n(i) \cdot e^{j2\pi \cdot n \cdot k/N_f} \,, \qquad (1)$$

where N_f denotes the used (I)FFT (or block) length, and $k \in \{-N_g, ..., 0, ..., N_f - 1\}$ the time index. It follows that one OFDM symbol consists of $N_g + N_f$ samples where N_g denotes a cyclic prefix as guard interval. Considering the sample rate f_s, the guard length is $T_g = N_g/f_s$, the FFT window length is $T_s = N_f/f_s$, and the total symbol duration is $T = (N_g + N_f)/f_s$. The guard interval should protect the received data against inter-symbol- (ISI) or inter-carrier-interference (ICI) in case of multipath propagation. It is a well known fact of OFDM, that the time domain signal $s(i,k)$ has a non-constant envelope, but there exist a lot of solutions to overcome this problem [22], [29], [42], [40], [39], [33].

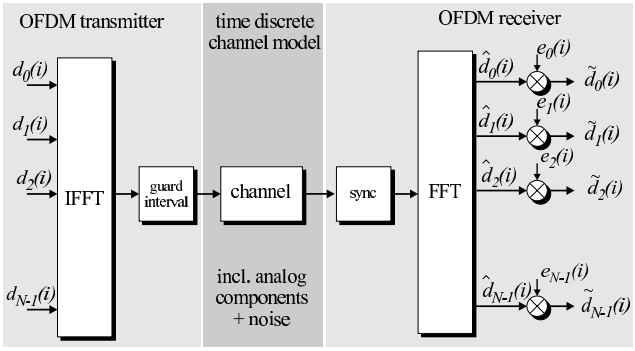

Fig. 1. Time discrete OFDM system

In general, each received symbol is influenced by all subcarriers of all OFDM symbols. If we assume the maximum channel delay time to be shorter than one OFDM symbol we only have ISI between the current (i) and the previous ($i-1$) OFDM symbol. The received symbols can be written as

$$\hat{d}_n(i) = \sum_{\mu=0}^{N-1} C_{n,\mu}^{(0)} \cdot d_\mu(i) + \sum_{\nu=0}^{N-1} C_{n,\nu}^{(-1)} \cdot d_\nu(i-1) \qquad (2)$$

where $\hat{d}_n(i)$ denotes the received symbol of the n^{th} subcarrier and C marks the frequency domain channel coefficient. Assuming time invariant conditions, the channel coefficients do not dependent on i, so that $C_{\mu,n}^{(0)}$ is a measure of ICI between the μ^{th} and n^{th} subcarrier of the i^{th} OFDM symbol. The second part of (2) is the ISI expressed by $C_{\nu,n}^{(-1)}$. For complete symbol detection a very complex equalizer has to be used. But, if the overall channel impulse response is not longer than the guard interval ($\tau_{\max} \leq T_g$), the channel influence can be described by a simple complex multiplication in frequency domain

$$\hat{d}_n(i) = C_n \cdot d_n(i) \,, \qquad (3)$$

where $C_n = C_{n,n}^{(0)}$. All other channel coefficients of $C_{\mu,n}^{(0)}$ and $C_{\nu,n}^{(-1)}$ are zero in case of ISI- and ICI-free-transmission. This is a very important aspect, because easy equalization (multiplication by $e_n = 1/C_n$ on each subcarrier separately) is one of the strongest assets of OFDM. This *zero forcing* solution is viable if channel state information is considered in the Viterbi channel decoder.

Thus, the guard time has to be longer than the maximum relative channel delay. The drawback of the guard interval is the bandwidth efficiency decreasing with the guard length. Since the guard interval contains no (new) information, the efficiency decreases by a factor of $(1 - T_g/T)$. Thus, for a proper design of an OFDM system a compromise between efficiency and additional ISI/ICI noise must be found. To minimize the ISI/ICI influence and the bandwidth efficiency loss, it is a possible solution to decrease the channel impulse response length by means of a linear pre-equalizer, like shown in section VI.

Concerning current WLAN standards, the total OFDM symbol duration is $T = 4\,\mu$s including a $T_g = 0.8\,\mu$s guard interval and the $T_s = 3.2\mu$s core symbol. The $N = 52$ active subcarriers are placed symmetrically about zero, with the DC component left blank. With a subcarrier distance of $\Delta f = 1/T_s = 312.5$ kHz the total OFDM bandwidth occupied is about 16.5 MHz. Using an $N_f = 64$ point FFT algorithm (oversampling rate $w = 1.23$), the required time domain sample rate is exactly $f_s = 20$ MHz. In combination with variable code rates (punctured convolutional codes) and different symbol mapping schemes (BPSK ... 64-QAM), the new WLAN standards provide data rates from 6 up to 54 Mbit/s.

III. Channel Estimation

As mentioned in the last section, the new WLAN standards HIPERLAN/2 and IEEE802.11a are based on the multi-carrier (MC) technique OFDM [18], [19], [21], [43] with coherent data demodulation. Channel estimation is required. In the PHY layer of both standards, different burst types with equal training symbols are defined. The preamble contains a synchronisation sequence of 8 μs (except the downlink burst) followed by 2 identical training symbols $d_n^P(i)$ (each 3.2 μs) and protected by one long guard interval (1.6 μs). The payload contains user data packets of 432 bit/packet. Figure 2 shows an example of a PHY burst (27 Mbit/s mode). Each data OFDM symbol consists of 48 data and 4 pilot carriers. The pilot carriers can be used for fine frequency tuning.

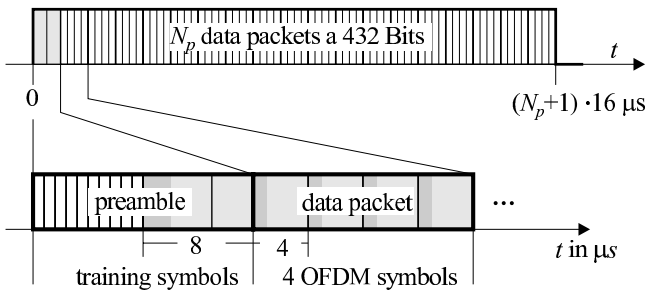

Fig. 2. Time domain burst structure (27 Mbit/s mode)

With the given burst structure, the system permits an estimation

using two subcarriers coefficients at the beginning of each burst

$$\hat{C}_n(i) = \frac{\hat{d}_n^P(i)}{d_n^P}. \tag{4}$$

With $|d_n^P(i)| = 1$, the division in (4) can be practically replaced with a multiplication by $(d_n^P)^*$. Assuming time invariant channels, the averaged coefficients are

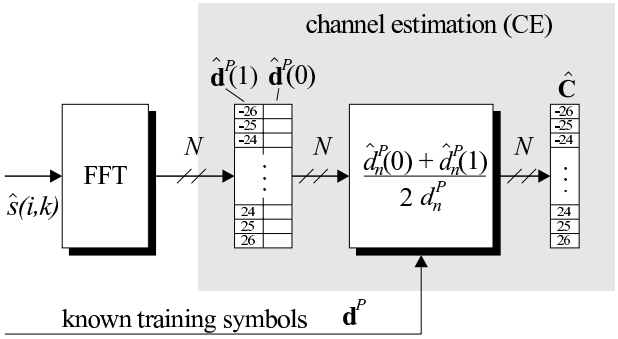

Fig. 3. Initial Channel estimation in frequency domain

$$\hat{C}_n = \frac{1}{2} \cdot (\hat{C}_n(0) + \hat{C}_n(1)). \tag{5}$$

Figure 3 shows the block diagram of the channel estimator. In case of AWGN the estimated coefficients are given by the true channel transfer coefficients C_n and additive noise N_n^{ce}

$$\hat{C}_n = C_n + N_n^{ce}, \tag{6}$$

where the averaged power of N_n^{ce} is 3 dB below the data symbol distortion (due to averaging over 2 pilot symbols). As simulation results will show, the presented channel estimation method results in an S/N loss of about 2 dB compared to simulations with perfectly known channels [36].
By exploiting the correlations between adjacent subcarriers coefficients, the estimator noise in (6) can be reduced substantially. The so-called *noise reduction algorithm* (NRA) is placed between IFFT and FFT as shown in figure 4.

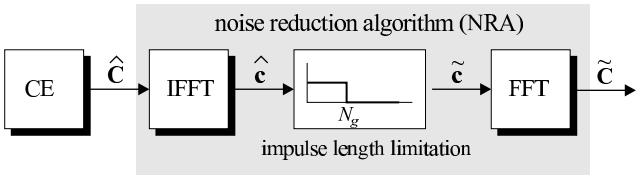

Fig. 4. Noise reduction algorithm (NRA)

In order to fulfill the condition of ISI and ICI free demodulation, the channel impulse response has to match the guard interval. In particular, the maximum channel delay must not exceed the guard time. With the number of guard samples N_g (here: 16), the channel impulse response vector $\mathbf{c}$ of one FFT block with length N_f satisfies

$$c(k) = 0 \quad ; \quad N_g \le k \le N_f - 1. \tag{7}$$

The estimated channel impulse response $\hat{\mathbf{c}}$ can be computed by an inverse fourier transformation of the estimated channel transfer function vector $\hat{\mathbf{C}}$

$$\hat{\mathbf{c}} = \mathbf{W}_{\mathrm{IDFT}} \cdot \hat{\mathbf{C}}, \tag{8}$$

with the IDFT matrix $\mathbf{W}_{\mathrm{IDFT}}$ containing all twiddle factors

$$W_{IDFT}(k,n) = \frac{1}{\sqrt{N_f}} \cdot e^{j2\pi \cdot n \cdot k / N_f}. \tag{9}$$

The basic idea of noise reduction is the limitation of the impulse response according to

$$\tilde{c}(k) = \begin{cases} \hat{c}(k) & ; \quad 0 \le k \le N_g - 1 \\ 0 & ; \quad N_g \le k \le N_f - 1 \end{cases}. \tag{10}$$

After re-transformation into frequency domain

$$\tilde{\mathbf{C}} = \mathbf{W}_{\mathrm{IDFT}^{-1}} \cdot \tilde{\mathbf{c}}, \tag{11}$$

the averaged noise power in $\tilde{C}_n$ has been reduced by the factor N/N_g. (note: if IDFT and DFT are used for noise reduction, the number of subcarriers N must be equal to the DFT length N_f. Another possibility will be presented in the following text.)

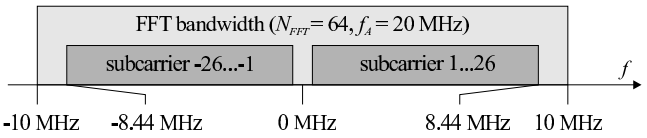

Fig. 5. Training symbols in frequency domain

The problem of this well-known technique is the computation of the IDFT (8) and the DFT (11) in case of incompletely estimated channel transfer functions. Some of the subcarriers cannot be estimated since they are not used (guard band, DC component, see figure 5) In order to overcome these problems, we can split the vector $\hat{\mathbf{C}}$ into subvector $\hat{\mathbf{C}}_\mathbf{k}$, containing all known or assessable coefficients and subvector $\hat{\mathbf{C}}_\mathbf{u}$ with all unknown channel coefficients. A similar split can also be done in time domain

$$\hat{\mathbf{c}}_\mathbf{1} = [\hat{c}(0), \hat{c}(1), ..., \hat{c}(N_g - 1)]^T, \tag{12}$$

$$\hat{\mathbf{c}}_\mathbf{0} = [\hat{c}(N_g), \hat{c}(N_g + 1), ..., \hat{c}(N_f - 1)]^T, \tag{13}$$

where $\hat{\mathbf{c}}_\mathbf{1}$ contains the true channel impulse response and $\hat{\mathbf{c}}_\mathbf{0}$ includes zeros (7) or pure noise. The IDFT can be computed by

$$\begin{bmatrix} \hat{\mathbf{c}}_\mathbf{1} \\ \hat{\mathbf{c}}_\mathbf{0} \end{bmatrix} = \begin{bmatrix} \mathbf{W_{11}} & \mathbf{W_{12}} \\ \mathbf{W_{21}} & \mathbf{W_{22}} \end{bmatrix} \cdot \begin{bmatrix} \hat{\mathbf{C}}_\mathbf{k} \\ \hat{\mathbf{C}}_\mathbf{u} \end{bmatrix}, \tag{14}$$

where the IDFT submatrices $\mathbf{W_{11}}$, $\mathbf{W_{12}}$, $\mathbf{W_{21}}$, and $\mathbf{W_{22}}$ include all N_f^2 twiddle factors (9) in a rearranged order. Due to a switched ranking within the frequency domain vector $\hat{\mathbf{C}}$, the rows of $\mathbf{W_k}$ have to be re-organized in the same way. Since $\hat{\mathbf{c}}_\mathbf{0} = \mathbf{0}$ according to (10), we get from (14)

$$\hat{\mathbf{c}}_\mathbf{0} = (\mathbf{W_{21}} \cdot \hat{\mathbf{C}}_\mathbf{k} + \mathbf{W_{22}} \cdot \hat{\mathbf{C}}_\mathbf{u}), \tag{15}$$

$$\mathbf{W_{22}} \cdot \hat{\mathbf{C}}_\mathbf{u} = -\mathbf{W_{21}} \cdot \hat{\mathbf{C}}_\mathbf{k}. \tag{16}$$

With a modified pseudo inverse $\mathbf{W_{22}^{+}}$

$$\underbrace{(\mathbf{W_{22}^{H}} \cdot \mathbf{W_{22}} + \gamma^{2} \cdot \mathbf{I})^{-1} \cdot \mathbf{W_{22}^{H}}}_{\mathbf{W_{22}^{+}}} \cdot \mathbf{W_{22}} = \mathbf{I}, \quad (17)$$

where $\mathbf{W^{H}}$ denotes the hermitean of $\mathbf{W}$, the unknown transfer factors can be computed by

$$\hat{\mathbf{C}}_{\mathbf{u}} = -\mathbf{W_{22}^{+}} \cdot \mathbf{W_{21}} \cdot \hat{\mathbf{C}}_{\mathbf{k}}, \quad (18)$$

with $\mathbf{I}$ the identity matrix. In order to prevent $\mathbf{W_{22}^{+}}$ from numerical instability, a small factor $0 < \gamma << 1/N_f$ has been introduced. The complete computation of $\hat{\mathbf{c}}_{\mathbf{1}}$ is

$$\hat{\mathbf{c}}_{\mathbf{1}} = \left(\mathbf{W_{11}} - \mathbf{W_{12}} \cdot \mathbf{W_{22}^{+}} \cdot \mathbf{W_{21}}\right) \cdot \hat{\mathbf{C}}_{\mathbf{k}}. \quad (19)$$

Considering (10)

$$\tilde{\mathbf{c}}_{\mathbf{1}} = \hat{\mathbf{c}}_{\mathbf{1}}, \quad (20)$$

$$\tilde{\mathbf{c}}_{\mathbf{0}} = \mathbf{0}, \quad (21)$$

and with the parts of the resorted DFT matrix

$$\begin{bmatrix} \tilde{\mathbf{C}}_{\mathbf{k}} \\ \tilde{\mathbf{C}}_{\mathbf{u}} \end{bmatrix} = \begin{bmatrix} \mathbf{W_{11}^{H}} & \mathbf{W_{21}^{H}} \\ \mathbf{W_{12}^{H}} & \mathbf{W_{22}^{H}} \end{bmatrix} \cdot \begin{bmatrix} \tilde{\mathbf{c}}_{\mathbf{1}} \\ \tilde{\mathbf{c}}_{\mathbf{0}} \end{bmatrix}, \quad (22)$$

it is possible to compute the noise reduced subcarrier coefficients

$$\begin{aligned} \tilde{\mathbf{C}}_{\mathbf{k}} &= \left[\mathbf{W_{11}^{H}} \cdot \left(\mathbf{W_{11}} - \mathbf{W_{12}} \cdot \mathbf{W_{22}^{+}} \cdot \mathbf{W_{21}}\right) \cdot \hat{\mathbf{C}}_{\mathbf{k}}\right] \\ &= \mathbf{W_{kk}} \cdot \hat{\mathbf{C}}_{\mathbf{k}}. \end{aligned} \quad (23)$$

Since the noise reduction matrix $\mathbf{W_{kk}}$ can be pre-computed, the noise reduction algorithm requires only one run-time matrix multiplication (23). Figure 6 depicts some simulation results of the 27 Mbit/s mode. For Monte-Carlo simulations, a typical Rayleigh fading indoor channel model with a delay spread $\Delta\tau$=100 ns has been chosen. As a reference, the results with perfectly known channel coefficients are given, too.

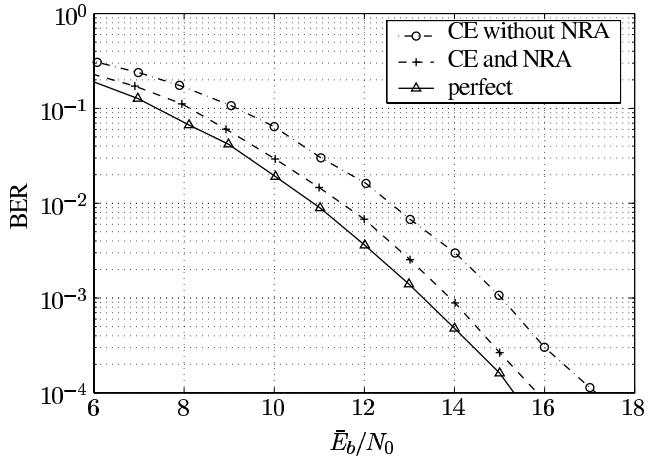

Fig. 6. Simulated bit error rates (BER) with channel estimation (CE) and noise reduction algorithm (NRA)

With raw channel estimation over 2 training symbols (CE without NRA), the E_b/N_0 loss is about 2 dB, compared to perfectly known channels. Using the noise reduction algorithm (23), the E_b/N_0 loss is reduced to 0.7 dB. For other HIPERLAN/2 or IEEE802.11a modes, similar results have been obtained.

IV. Channel tracking

The HIPERLAN/2 and IEEE802.11a standards provide 2 training symbols in front of each data burst and 4 pilot carriers inside each data symbol. In case of time variant channel coefficients, the initial channel estimation suffices only for OFDM symbols near the beginning of the burst. Therefore only 4 pilot carriers are not sufficient to supply channel tracking for a complete subcarrier coefficient set [26], [27], [28].

In order to create additional training symbols, received and decided data can be re-modulated to re-estimate the channel coefficients during data demodulation, as it can be seen in figure 7. The best choice would be decided data feedback from the Viterbi decoder output, because the bit error rate (BER) is much better than at the decoder input. However, code termination is only provided at the end of each data burst. Before code termination has been reached, a sufficiently safe data decision will be at the expense of some Viterbi decision delay. Figure 8 shows the simulated bit error rates subjected to the Viterbi decoding delay $k_{\max}$ with different coding rates R_p.

The results of figure 8 are summarized in table I for all HIPERLAN/2 modes. In a worst case scenario with $R_p = 3/4$, the Viterbi decoder needs a delay of 100 decoded bits. With one OFDM symbol containing 36 data bits (9 Mbit/s mode), a maximum decoding delay of $i_0 = 3$ complete OFDM symbols is required. In order to obtain comparable results, this delay has been used for all modes.

The other feedback possibility is to use the non decoded symbols at the symbol decoder output for re-modulation ($i_0 = 0$). Figure 7 illustrates both options.

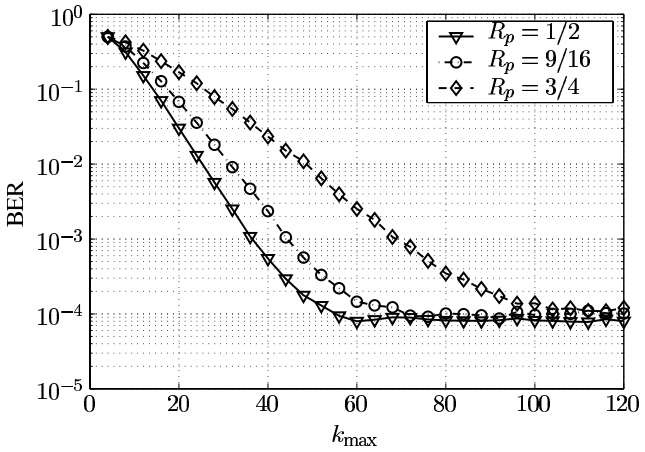

Fig. 8. Simulated bit error rates (BER) of 27 Mbit/s mode versus decoding delay $k_{\max}$ (only AWGN)

The first $i_0 + 1$ OFDM symbols are demodulated by using the initial channel estimate. The decided data (before or after decoding) must be re-modulated. The decision delay is denoted

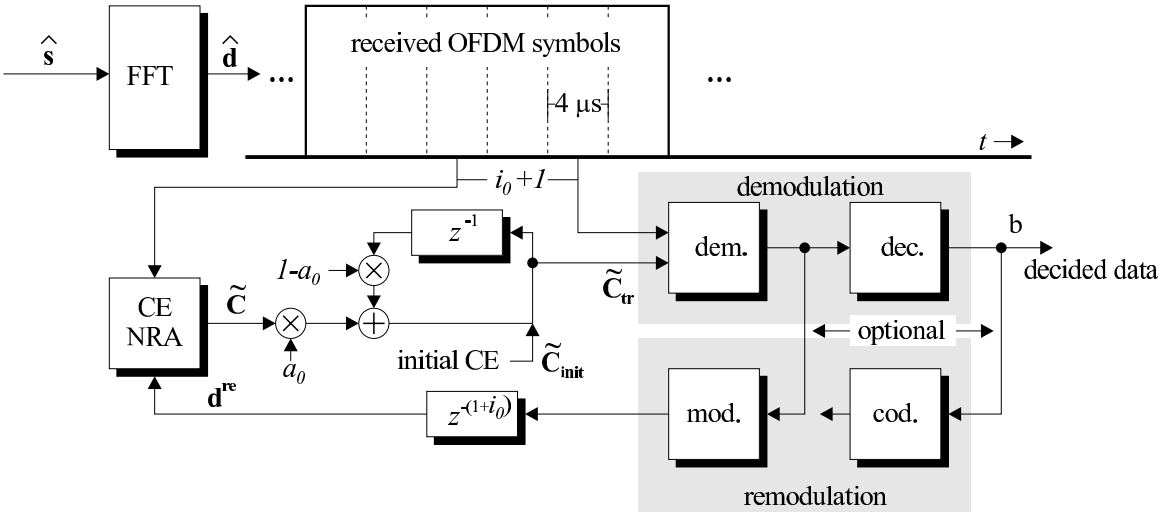

Fig. 7. Block diagram of decision directed channel tracking

Mode	R_b	N_{bps}	$k_{\max}$	$\min(i_0)$	Δt_{dec}
6	1/2	24	>60	3	12 μs
9	3/4	36	>110	3	12 μs
12	1/2	48	>60	2	8 μs
18	3/4	72	>110	2	8 μs
27	9/16	108	>70	2	8 μs
36	3/4	144	>110	1	4 μs
54	3/4	216	>120	1	4 μs

TABLE I
Estimated decoding delay

by $z^{-(1+i_0)}$. Dividing $\hat{\mathbf{d}}(i)$ by $\mathbf{d^{re}}(i)$ and applying the noise reduction algorithm will produce a new channel estimate $\tilde{\mathbf{C}}(\mathbf{i})$ for the i^{th} OFDM symbol. In order to reduce noise influence, a first order loop filter with parameter $a_0 < 1$ has been introduced, as shown in figure 7.

Finding an optimal loop parameter a_0 means a compromise between noise sensitivity and tracking ability. In order to simulate the noise influence, a time-invariant Rayleigh-fading indoor channel model ($\Delta\tau = 100$ns) has been used. Figure 9 shows the simulated BER versus a_0 for both cases: decided data feedback before (uncoded) and after Viterbi decoding (coded). The averaged noise power is $\bar{E}_b/N_0 = 15$ dB.

In case of $a_0 = 0$, no tracking is applied and the BER must therefore be identical to that in figure 6 with NRA. Of course, with an increased a_0, the noise influence on tracking based on non-decoded reference symbols rises more than for decoded symbols. With $a_0 < 0.2$ (uncoded) and $a_0 < 0.5$ (coded) a negligible BER loss is obtained.

For tracking power simulations, a time variant channel model has been used, considering Jakes-distributed Doppler-spreading derived from mobile speed $v_{\max}$

$$f_{D,\max} \approx \frac{1}{\lambda} \cdot v_{\max} \tag{24}$$

with wave length $\lambda = \frac{c_0}{f_0}$ (here $\lambda = 5.77 \cdot 10^{-2}$m).

In figure 10 the simulated packet error rates (PER) of a HIPER-

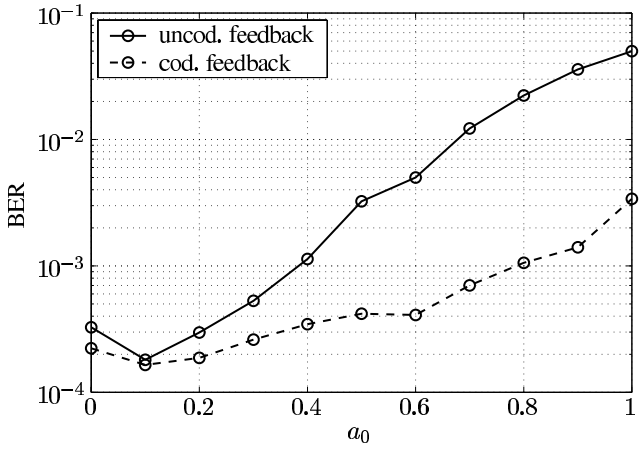

Fig. 9. Simulated bit error rates (BER) of 27 Mbit/s mode versus loop parameter a_0 with $\bar{E}_b/N_0 = 15$dB}

LAN/2 system (27 Mbit/s) in case of high mobility is depicted. The simulated PHY burst length is about 800 μs. Without tracking, the PER becomes very high for more than 3 m/s. Applying channel tracking after exploiting Viterbi decoding, the system functionality can be guaranteed up to $v_{\max} = 30$ m/s.

V. A Comparison to Single-Carrier Frequency-Domain Equalizer

One typical charateristic of OFDM is channel equalization by multiplying each subcarrier separately. The cyclic prefix allows to handle the received signal as periodic, i.e. to apply cyclic convolution. Thus, the DFTs of the signal and the channel impulse response can be multiplied (3).

Single-carrier systems with frequency domain equalizer (SC-FEq) [37], [38] draw on the same idea. Since both systems, OFDM and SC-FEq, have similar equalization structures, the frequency domain equalizer will be explained and compared to OFDM in this section.

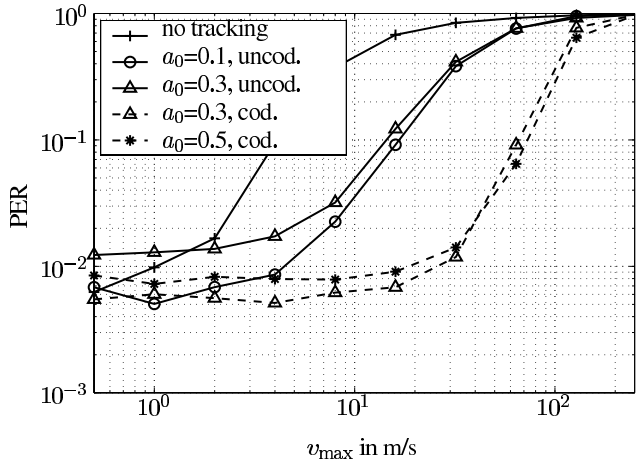

Fig. 10. Simulated packet error rates (PER) of 27 Mbit/s mode versus object speed v_{max} with $\bar{E}_b/N_0 = 15$

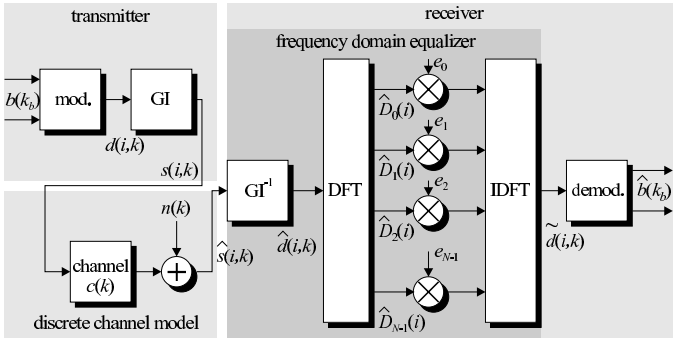

Fig. 11. Block diagram of SC-FEq system

The block diagram of a single-carrier system with linear frequency domain equalizer is given in figure 11. The modulated data $d(i,k)$ are divided into blocks of FFT length N_f, where i is the block index and $k = 0, 1, ..., N_f - 1$. Each block gets a cyclic prefix containing the last N_g data symbols of each block. If the discrete channel impulse response $c(k)$ matches the guard interval, the received blocks $\hat{d}(i,k)$ consist of the cyclic convolution of $d(i,k)$ and $c(k)$ disturbed by white Gaussian noise $n(i,k)$

$$\hat{d}(i,k) = n(i,k) + \sum_{\mu=0}^{N_g} c(\mu) \cdot d(i, \mathrm{mod}(k-\mu, N_f)) \,. \quad (25)$$

The discrete fourier transform (DFT) of each block is

$$\hat{D}_n(i) = \sum_{k=0}^{N_f-1} \hat{d}(i,k) \cdot e^{-j2\pi \cdot n \cdot k/N_f} \quad (26)$$

$$= D_n(i) \cdot C_n + N_n(i) \,. \quad (27)$$

Due to this simple multiplicative channel influence, equalization can be performed in same way as in OFDM systems

$$\tilde{D}_n(i) = e_n \cdot \hat{D}_n(i) \,. \quad (28)$$

After inverse fourier transform (IDFT), the received and equalized data symbols are given by

$$\tilde{d}(i,k) = \frac{1}{N} \sum_{n=0}^{N_f-1} e_n \cdot \hat{D}_n(i) \cdot e^{j2\pi \cdot n \cdot k/N_f} \quad (29)$$

Without noise, the transmitted spectrum of each block $D_n(i)$ can be perfectly recomputed via $e_n = 1/C_n$. This so-called *zero forcing* solution (ZF) is optimum in noise free cases, only. On the other hand, in the presence of noise, the noise amplification of the ZF equalizer

$$A_{ZF} = \frac{1}{N} \cdot \sum_{n=0}^{N_f-1} \frac{1}{|C_n|^2} \quad (30)$$

could increase up to infinity, if $|C_n|$ becomes zero. To minimize the total error, considering ISI and noise amplification, the well-known MMSE solution can be used to compute the equalizer coeffizients

$$e_{n,MMSE} = \frac{1}{C_n + \frac{1}{\gamma_m^2 \cdot C_n^*}} \,, \quad (31)$$

where γ_m^2 denotes the mean signal to noise ratio. The remaining noise amplification decreases to [38]

$$A_{MMSE} = \frac{1}{N} \cdot \sum_{n=0}^{N_f-1} \frac{1}{|C_n|^2 + \frac{1}{\gamma_m^2}} \leq A_{ZF} \,. \quad (32)$$

For comparison of SC-FEq and OFDM a simulation system with same blocklength $N_f = 96$ (different from HIPERLAN/2 or IEEE802.11a), same guard length ($N_g = 16$), same signal mapping (QPSK), and a discrete slow-fading indoor-channel-model has been used. The simulation results of both systems without channel coding can be seen in figure 12.

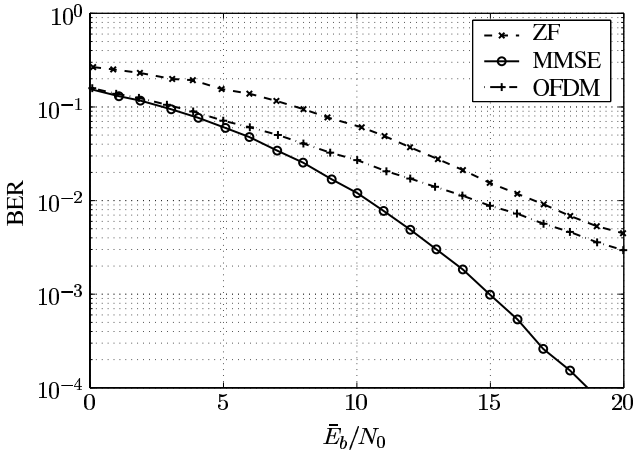

Fig. 12. Comparison of OFDM and SC-FEq without channel coding

The OFDM system and the ZF-SC-FEq system suffer considerably from noise amplification. Only the MMSE-SC-FEq equalizer makes use of frequency domain diversity and can reduce the BER enormously. But in practical systems, OFDM will be

always combined with channel coding, thus a half-rate convolutional channel coding with Viterbi-decoding and block interleaving (length 192) are added to both systems. The resulting bit-error-rates are shown in figure 13.

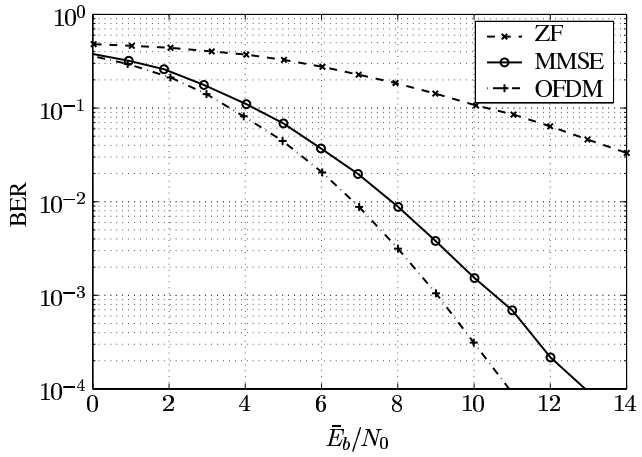

Fig. 13. Comparison of OFDM and SC-FEq with half-rate convolutional channel coding

While the BER of the ZF-SC-FEq equalizer is even worse by applying channel coding, the performance of the coded MMSE-SC-FEq system is about 4 dB better compared to the uncoded case. Channel coding has the most beneficial effect for OFDM; as shown in figure 13, the OFDM performance is better than the performance of MMSE-SC-FEq (almost 2 dB). This can be explained as follows: In the SC-FEq system each data bit occupies the full bandwidth: the reliability is uniformly distributed over all subcarriers. In contrast, in OFDM systems each bit is connected with an individual subcarrier – the reliability is different due to frequency selective, Rayleigh distributed channel coefficients. In this case, Viterbi decoding is more efficient than in case of uniformly weighted channel state information.

VI. Impulse Shortening Techniques

In section II it was mentioned, that it is an important goal to reduce the length of the guard interval in case of extremly long channel echo durations. A simplified OFDM block diagram including a time-domain pre-equalizer for impulse shortening is shown in figure 14.

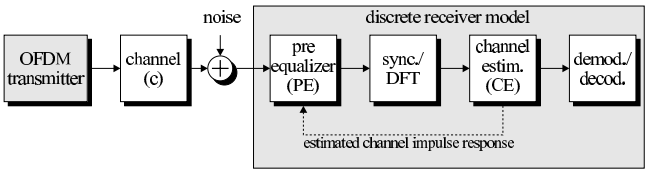

Fig. 14. Block diagram of OFDM system

After leaving the transmitter, the OFDM signal passes a slowly fading channel, represented by a discrete block 'channel'. All characteristics of necessary components like digital/analog conversion (DAC), baseband to bandpass conversion, etc. are described by the discrete vector

$$\mathbf{c} = [c(0), c(1), c(2), ..., c(m)]^T . \tag{33}$$

We assume that $m > N_g$. If not, impulse truncation is unnecessary because the guard interval can eliminate the influence of multipath propagation completely. All other noise influences are modelled by additive white Gaussian noise (AWGN). The time domain pre-equalizer for impulse truncation is placed before synchronization (positioning the FFT window) and DFT computation. If an FIR filter is used, the pre-equalizer is described by

$$\mathbf{e} = [e(0), e(1), e(2), ..., e(p)]^T . \tag{34}$$

Further on we exploit the fact, that the convolution $\mathbf{c_e} = \mathbf{c} * \mathbf{e}$ leads to an impulse length $(m + p + 1)$ with the first and last elements of $\mathbf{c}$ and $\mathbf{e}$ being non-zero

$$\mathbf{c_e} = [c_e(0), c_e(1), c_e(2), ...c_e(p + m - 1)]^T . \tag{35}$$

Figure 15 shows schematically the channel impulse response before and after applying the pre-equalizer. To get the new impulse response $\mathbf{c_e}$, we have to minimize the power of all elements $c_e(k)$, with $k > N_g$.

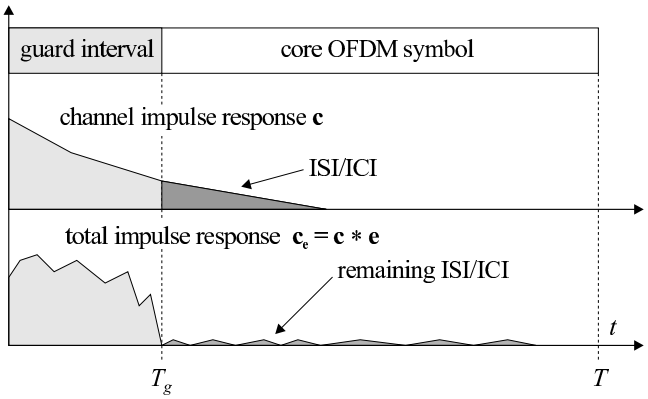

Fig. 15. Impulse response before and after pre-equalizing

Using well-known MMSE algorithms for developing T-equalizers [35], we have to create a convolution matrix $\mathbf{F}$, which has a Toeplitz structure and contains the samples of the channel impulse response of size $((m + p + 1) \times (p + 1))$

$$\mathbf{F} \cdot \mathbf{e} = \mathbf{c_e} . \tag{36}$$

As for $\mathbf{c_e}$, following constraints apply:

$$c_e(k) = \begin{cases} 1 & k = 0 \\ \star & 0 < k \leq N_g \\ 0 & k > N_g \end{cases} . \tag{37}$$

The condition $c_e(0) = 1$ is necessary to prevent an all-zero solution; of course any non-zero complex value can be assumed for $c_e(0)$. Since all elements indexed by $k = \{1, ..., N_g\}$ and signed by $\star$ are non-relevant, we may restrict the conditions for $\mathbf{c_e}$ by excluding all arbitrary elements:

$$c_{re}(k) = \begin{cases} 1 & k = 0 \\ 0 & k \geq 1 \end{cases} . \tag{38}$$

According to (37) and (38), a new reduced convolution matrix $\mathbf{F_r}$ of size $((p+m+1-N_g)\times(p+1))$ can be defined

$$\mathbf{F_r}\cdot\mathbf{e}=\mathbf{c_{re}}\,, \tag{39}$$

where $\mathbf{F_r}$ is equal to $\mathbf{F}$ except for the lines with indices $\{1,...,N_g\}$. With (38), we have to find an equalizer $\mathbf{e}$ fulfilling

$$\mathbf{F_r}\cdot\mathbf{e}=\mathbf{d}+\delta\,. \tag{40}$$

The desired vector

$$\mathbf{d}=[1,0,....,0]^T \tag{41}$$

results from (38) and the error vector

$$\delta=[\delta(0),\delta(1),\delta(2),...,\delta(p+m-N_g)]^T \tag{42}$$

describes the remaining error, which has to be minimized. A well known solution for equations like (39) is the minimum mean square error (MMSE) technique [35], [34], so the equalizer can be computed by

$$\mathbf{e}=(\mathbf{F_r}^{\mathrm{H}}\cdot\mathbf{F_r})^{-1}\cdot\mathbf{F_r}^{\mathrm{H}}\cdot\mathbf{d}\,. \tag{43}$$

Just channel knowledge to create $\mathbf{F_r}$ and the trivial destination vector $\mathbf{d}$ are required to compute the FIR equalizer coefficients. Since in case of additional noise (AWGN), the pre-equalizer will raise the noise power; optimal MMSE solutions take the effective signal to noise ratio (SNR) into account

$$\mathbf{e}=(\mathbf{F_r}^{\mathrm{H}}\cdot\mathbf{F_r}+\gamma^2_{\mathbf{pe}}\cdot\mathbf{I})^{-1}\cdot\mathbf{F_r}^{\mathrm{H}}\cdot\mathbf{d}\,, \tag{44}$$

with γ^2_{pe} = 1/SNR and the identity matrix $\mathbf{I}$. To demonstrate the functionality of (43), a short example is introduced. We assume a channel impulse response $c(k)$ of length $m+1=15$ shown in figure 16a. Thus, $c(k)$ has 15 non-zero coefficients. Further on, we assume a guard interval of length $N_g=8$.

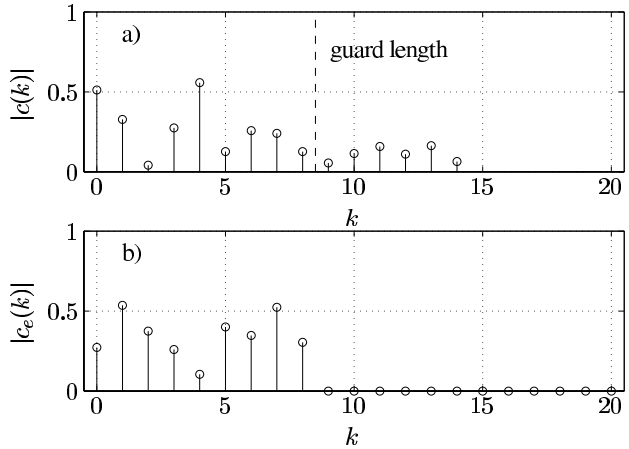

Fig. 16. a) Channel impulse response c(k); b) Convolution of channel impulse response and pre-equalizer

In this example, no additional noise is added ($\gamma^2_{pe}=0$). The convolution of the channel $c(k)$ and the computed FIR pre-equalizer $e(k)$ with order $p=31$ is shown in figure 16b. It can be clearly seen, that the result of pre-equalizing contains quasi-zero coefficients for $k>8$.

Figure 17 shows the results of some statistical analyses. The total power delay profiles of truncated channel impulse responses are shown. This figure is based on more than 5000 random channels with an exponential power delay profile and average delay spread $\Delta\tau=250$ns. The remaining ISI/ICI decreases by raising the pre-equalizers size p. Again, no noise and the ideal channel knowledge have been assumed.

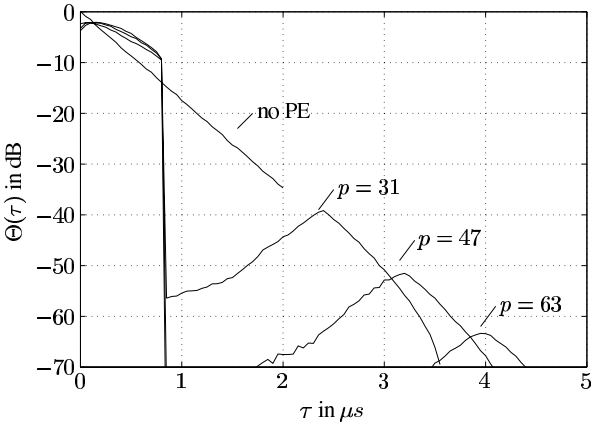

Fig. 17. Power delay spectrum of the total channel impulse response $(c_e(k), \Delta\tau=250\text{ns})$ with different pre-equalizer lengths

The fundamental equation (44) for the pre-equalizer MMSE-solution is based on channel knowledge. In practical systems, a channel estimation in time or frequency domain is required for coherent demodulation.

As explained in section III, the indoor communication standard HIPERLAN/2 contains two training-symbols in order to perform frequency domain channel estimation. To prevent ISI/ICI-disturbance in case of insufficient guard length, the training-symbols are provided with a double length guard interval (GI2). In figure 18a the training structure of a HIPERLAN/2 burst is shown [18], [21].

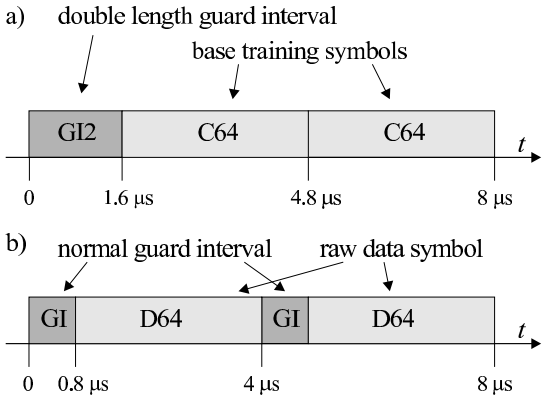

Fig. 18. a) Training symbols and double length guard interval; b) "Normal" data OFDM symbols

The two equal base training symbols (C64) consist of each 64 samples (20 MHz sample frequency). With a guard length of 32, it is possible to estimate channels up to length 32 without ISI/ICI-disturbance. If the estimated channel impulse response

is longer than the guard interval length of normal data OFDM symbols – the standard provides a guard length of 16 samples (800 ns) – we have to compute a pre-equalizer (44) to truncate the effective impulse length of channel and pre-equalizer filter.

As it was mentioned in section III, the training structure of HIPERLAN/2 allows to estimate 52 subcarriers coefficients $\hat{C}_n$. To compute the channel impulse response, we assume a maximum channel impulse response length $m+1$ (length of $\tilde{\mathbf{c}}^{\mathbf{1}} = 32$). Similar to (14), the required channel impulse response $\tilde{\mathbf{c}}^{\mathbf{1}}$ can be computed by

$$\hat{\mathbf{c}}^{\mathbf{1}} = \left(\mathbf{W_{11}} - \mathbf{W_{12}} \cdot \mathbf{W_{22}^{+}} \cdot \mathbf{W_{21}}\right) \cdot \hat{\mathbf{C}}^{\mathbf{k}} \quad (45)$$

$$= \mathbf{W_{1k}} \cdot \hat{\mathbf{C}}^{\mathbf{k}} \quad (46)$$

By pre-computing the $((m+1) \times q)$ matrix $\mathbf{W_{1k}}$, the runtime costs are only a vector/matrix multiplication (46). With (44) the pre-equalizer can be computed and used after initial channel estimation. The new transfer function of the complete impulse response $\mathbf{c_e}$ can be computed in frequency domain by multiplying $\tilde{\mathbf{C}}$ and DFT $\{\mathbf{e}\}$.

The pre-equalizer is not needed as long as the channel impulse response does not exceed the guard length. In this case, there is no advantage for applying a FIR pre-equalizer.

To show the effect of the pre-equalizer under realistic conditions, a sensitive mode (54 Mbit/s) and a very dispersive channel have been chosen. The complex symbols on each subcarrier are taken form the 64-QAM alphabet and the required error protection is handled by a R=3/4 punctured convolutional code. The block interleaver size is 288; this deals with the number of coded bits per OFDM symbol. The channel coefficients used are based on a channel estimation, considering the training structure of HIPERLAN/2 by a simple least squares estimation without applying the noise reduction algorithm (NRA). In our simulations, we used data packets of length 432 bits. A packet error occurs, if only one bit is wrong after viterbi decoding. In a real system defective packets have to be transmitted again.

The used mobile radio channel is based on a channel model, developed in connection with HIPERLAN/2 standardization. This channel models contain 5 different exponential power delay profiles with delay spreads from 50 ns up to 250 ns. To demonstrate the effect of pre-equalizing, we used the channel type E ($\Delta\tau = 250$ ns).

From section VI, pre-equalization can be expected to yield a substantial gain. One possibility to overcome the problems of channel estimation is the technique described in section VI. In particular, equation (46) is fundamental in exploiting the training-symbol based OFDM channel estimation of HIPERLAN/2.

Before we may start channel estimation, the maximum channel impulse response length must be fixed for pre-computing $\mathbf{W_{1k}}$. Here, we assumed a channel length $(m+1) = 36$, so $\mathbf{W_{1k}}$ becomes a matrix with dimensions (36×52). In figure 19 the simulation results are shown. In case of no pre-equalizer (no PE), a very high error floor is the consequence of ISI and ICI. For the sake of completeness, the case of pre-equalizing with perfectly known channel impulse response is depicted in figure 19, too (PE, no CE). If we consider a realistic channel estimation (PE and CE), the SNR performance loss is < 1 dB (at PER 10^{-2}) with respect to the perfectly known channel case.

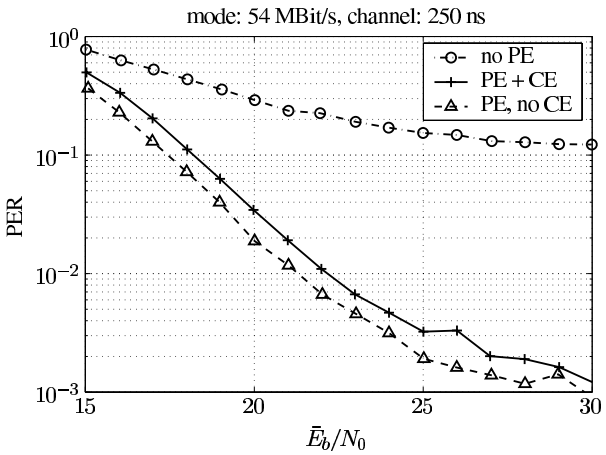

Fig. 19. Packet error rate without pre-equalization (PE), with pre-equalization and ideal known channel impulse response (PE, no CE), and pre-equalization with training symbol based channel estimation (PE and CE)

VII. Conclusion

In this paper some algorithms where discussed which improve the performance of OFDM systems. For channel estimation a specific noise reduction method is presented which takes into account that sometimes not all subcarriers are modulated – this is the case for example in HIPERLAN/2. In this standard two training symbols at the beginning of each data block are used for channel estimation. In case of large burst lengths problems may arise even for moderate time variance. To solve this problem a channel tracking algorithm based on the modern turbo principle is developed. In former papers, single carrier receiver structures with frequency domain equalizers were concidered which look quite similar to the OFDM configuration. In this paper a comparison of both alternatives is given which shows that OFDM outperforms the single carrier structure if channel coding is included. Finally, the problem of channel echo overlength is addressed; it is shown that by the application of a linear pre-equalizer the impulse response in most cases can be limited below the guard interval length.

As explained, ODFM is a very attractive solution for mobile radio applications – another favorite in this field is the CDMA concept (Code Division Multiple Access) which is applied in the 3rd generation standard UMTS. In several recent papers a *combination* of both favorites has been suggested [44], [45]. In this new modulation scheme called *Multicarrier-CDMA* or *Multicarrier Spread-Spectrum* the advantages of both concepts are connected. Future research will be focused on this attractive new technique.

References

[1] M. Doelz. *Binary Data Transmission Technique for Linear Systems.* Proc. IRE, May, 1957. S.656-661.

[2] B. R. Saltzberg. *Performance of an Efficient Parallel Data Transmission Scheme.* IEEE Trans. on Communications, COM-15 Nr. 6, 1967. S.805-811.

[3] S. Weinstein and P. M. Ebert. *Data Transmission by Frequency-Division Multiplexing Using the Discrete Fourier Transform.* IEEE Trans. on Communications, COM-19 Nr. 5, October, 1971. S.628-634.

[4] H.-J. Kolb. *Untersuchungen über ein digitales Mehrfrequenzverfahren zur Datenübertragung.* PhD Thesis, University of Erlangen-Nürnberg, Erlangen, 1981.

[5] H.W. Schüßler. *Ein digitales Mehrfrequenzverfahren zur Datenüber-*

tragung. Stand und Entwicklungsaussichten der Daten- und Textkommunikation. Professorenkonferenz im FTZ, 1983.

[6] R. Rückriem. *Realisierung und meßtechnische Untersuchungen an einem digitalen Parallelverfahren zur Datenübertragung im Fernsprechkanal*. PhD Thesis, University of Erlangen-Nürnberg, Shaker Verlag, April 1985.

[7] J.A. Bingham. *Multicarrier Modulation for Data Transmission: An Idea whose Time has come*. IEEE Comm. Magazine, May 1990. S.5-14.

[8] W.Y. Zou and Y. Wu. *COFDM: An Overview*. IEEE Trans. on Broadcasting, 41(1), March 1995. S.1-8.

[9] K. D. Kammeyer, H. Schulze, U. Tuisel, and H. Bochmann. *Digital Multicarrier-Transmission of Audio Signals Over Mobile Radio Channels*. In Proc. ETT-92, 1992. Vol.3, page 23-33.

[10] U. Tuisel. *Multiträgerkonzepte für die digitale, terrestrische Hörrundfunkübertragung*. PhD Thesis, TU Hamburg-Harburg, 1993.

[11] S.D. Sandberg and M.A. Tzannes. *Overlapped Discrete Multitone Modulation for High Speed Copper Wire Communications*. IEEE J. on Sel. Areas in Comm., 13(9), December, 1995. S.1571-1585.

[12] K. Matheus. *Generalized Coherent Multicarrier Systems for Mobile Communications*. PhD Thesis, University of Bremen, Arbeitsbereich Nachrichtentechnik, Shaker Verlag, Juni 1998.

[13] K. Matheus, K.D. Kammeyer, and U. Tuisel . *Implementation of Multicarrier Systems with Polyphase Filterbanks*. Proc. of MCSS, Oberpfaffenhofen 1999.

[14] U. Reimers. *Digitale Fernsehtechnik*. Springer-Verlag, 1995.

[15] A. Vahlin and N. Holte. *OFDM for Broadcasting in Presence of Analoque Co-Channel Interference*. IEEE Trans. on Broadcasting, 41(3), September, 1996. S.89-93.

[16] T. de Courville, R. Monnier, and J.B.Rault. *OFDM for digital TV broadcasting*. Signal Processing, 39, September, 1994. S.1-32.

[17] Sony International (Europe) GmbH. *BDMA, the Multiple Access Scheme Proposal for the UMTS Terrestrical Radio Air Interface (UTRA)*. ETSI SMG2 Concept Group Meeting – OFDM Concept Group 39, London, Heathrow, UK, June, 1997.

[18] ETSI. HIPERLAN Type 2 Functional Specification Part 1 – Physical PHY Layer. Technical Report DTS/BRAN030003-1, ETSI EP BRAN, April, 2000.

[19] IEEE. Draft Supplement to STANDARD for Information Technology-Telecommunications and information exchange between systems – Local and metropolitan area networks – Specific Requirements – Part 11: Wireless LAN Medium Access Control MAC and Physical Layer PHY specifications: High Speed Physical Layer in 5 GHz Band. Technical Report IEEE P802.11a/D7.0, IEEE, 1999.

[20] G. Dickmann. *Analyse und Anwendung des DMT-Mehrträgerverfahrens zur digitalen Datenübertragung*. PhD Thesis, TU Hamburg-Harburg, VDI-Verlag, Düsseldorf, November 1997.

[21] M. Johnsson. HiperLAN/2 - The Broadband Radio Transmission Technology Operating in the 5 GHz Band. *HiperLAN/2 Global Forum (www.hiperlan2.com)*, 1999. Version 1.0.

[22] M. Friese. OFDM Signals with low Crest Factor. In *Proc. IEEE Global Telecommun. Conf. (GLOBECOM)*, 1997.

[23] H. Meyr, M. Moeneclaey, and S. A. Fechtel. *Digital Ccommunication Receivers*. John Wiley, 1. edition, 1998.

[24] P. Hoeher, S. Kaiser, and P. Robertson. Two-dimensional pilot-symbol-aided channel estimation in OFDM systems. *Proc. GLOBECOM-97*, November 1997. S.1845-1848.

[25] M. Bossert, A. Donder, and V.Zyablov. *Coded modulation for OFDM on mobile radio channels*. In *EPMCC*-97, 3. ITG-Fachtagung *Mobile Kommunikation* in Bonn, Germany, 1997, S.109-116.

[26] M. Bossert, A. Donder, and V.Zyablov. *Improved channel estimation with decision feedback for OFDM systems*. Electronic Letters, Vol.34 (Nr.11), May, 1998, S.1064-1065.

[27] A. Donder. *Beiträge zur OFDM-Übertragung im Mobilfunk*. PhD Thesis, University of Ulm, VDI, Juli 1999.

[28] M. Feuersänger, H. Schmidt, and K.D. Kammeyer. An Iterative Channel Estimation for a Hiperlan/2 OFDM System. In *Proc. of 5. international OFDM Workshop*, Hamburg-Harburg, Germany, September 2000.

[29] H. Schmidt and K.D. Kammeyer. Adaptive Subcarrierselektion zur Verringerung der Spitzenwerte eine Multiträger-Signals. Technical Report: Nr. 197 55 632.9 / Bosch EM 97/3099, Deutsche Patentanmeldung, Dezember 1997.

[30] H. Schmidt and K.D. Kammeyer. Reducing the Peak to Average Power Ratio of Multicarrier Signals by Adaptive Subcarrier Selection. In *Proc. IEEE International Conf. on Universal Personal Communications (ICUPC)*, Florence, Italy, October 1998.

[31] H. Schmidt and K.D. Kammeyer. Quantization and its Effects on OFDM Concepts for Wireless Indoor Applications. In *Proc. of 1st international OFDM Workshop*, Hamburg-Harburg, Germany, September 1999.

[32] H. Schmidt and K.D. Kammeyer. Impulse Truncation for Wireless OFDM Systems. In *Proc. of 5. international OFDM Workshop*, Hamburg-Harburg, Germany, September 2000.

[33] H. Schmidt. *OFDM für die drahtlose Datenübertragung innerhalb von Gebäuden*. PhD thesis, University of Bremen, Arbeitsbereich Nachrichtentechnik, Shaker Verlag, April 2001.

[34] K. D. Kammeyer. Time Truncation of Channel Impulse Responses by Linear Filtering. *AEÜ*, Vol.48(5), 1994.

[35] K. D. Kammeyer. *Nachrichtenübertragung*. B.G.Teubner, Stuttgart, 2. edition, 1996.

[36] H. Schulze. *The Performance of a Coded Multicarrier 64-QAM System with Channel Estimation*. In *Proc. of 1st international OFDM Workshop*, Hamburg-Harburg, Germany, September 1999.

[37] H. Sari, G. Karam, and I. Jeanclaude. *An Analysis of Orthogonal Frequency Division Multiplexing for Mobile Radio Applications*. In *Proc. VTC-94*, Stockholm, Sweden, 1994. S.1635-1639.

[38] M. Huemer. *Frequenzbereichsentzerrung für hochratige Einträger-Übertragungssysteme in Umgebungen mit ausgeprägter Mehrwegeausbreitung*. PhD Thesis, University of Linz, November 1999.

[39] S. Müller-Winfurtner. *OFDM for Wireless Communications*. PhD Thesis, University of Erlangen-Nürnberg, Shaker Verlag, April 2000.

[40] M. Pauli. *Zur Anwendung des Mehrträgerverfahrens OFDM mit reduzierter Außerbandstrahlung im Mobilfunk*. PhD Thesis, University of Hannover, Institut für Allgemeine Nachrichtentechnik, VDI, Juni 1999.

[41] H. Rohling and R. Grünheid. Performance of an OFDM-TDMA Mobile Communication System. In *Proc. VTC-96*, 1996.

[42] T. May and H. Rohling. Reduktion von Nachbarkanalstörungen in OFDM-Funkübertragungssystemen. In *OFDM-Fachgespräch 1997, Brauschweig*, 1997.

[43] R. van Nee and R. Prasad. *OFDM for Wireless Multimedia Communications*. Artech House Publishers, Boston, London, 2000.

[44] A. Dekorsy. *Kanalcodierungskonzepte für Mehrträger-Codemultiplex in Mobilfunksystemen*. PhD thesis, University of Bremen, Arbeitsbereich Nachrichtentechnik, Shaker Verlag, July 2000.

[45] K. Fazel and S. Kaiser (Editor) *Multi-Carrier Spread-Spectrum — Related Topics*. Kluver Academic Publisher, 2000.